Received 5 January 2018; revised 6 April 2018; accepted 16 April 2018. Date of publication 25 April 2018; date of current version 31 August 2018.
The review of this paper was arranged by Editor M. Nafría.

Digital Object Identifier 10.1109/JEDS.2018.2829933

A Physical Model for the Hysteresis in MoS_2 Transistors

THERESIA KNOBLOCH [1], GERHARD RZEPA [1], YURY YU. ILLARIONOV [1,2], MICHAEL WALTL [1], FRANZ SCHANOVSKY [3], BERNHARD STAMPFER [1], MARCO M. FURCHI [4], THOMAS MUELLER [4], AND TIBOR GRASSER [1] (Fellow, IEEE)

1 Institute for Microelectronics, TU Wien, 1040 Vienna, Austria
2 Division of Solid State Electronics, Ioffe Physical-Technical Institute, Saint Petersburg 194021, Russia
3 Global TCAD Solutions, 1010 Vienna, Austria
4 Institute for Photonics, TU Wien, 1040 Vienna, Austria

CORRESPONDING AUTHOR: T. KNOBLOCH (e-mail: knobloch@iue.tuwien.ac.at)

This work was supported in part by FWF under Grant I2606-N30, and in part by the European Union Graphene Flagship under Grant 696656.

ABSTRACT Even though the hysteresis in the gate transfer characteristics of two-dimensional (2D) transistors is a frequently encountered phenomenon, the physics behind it are up to now only barely understood, let alone modeled. Here, we demonstrate that the hysteresis phenomenon can be captured accurately by a previously established non-radiative multiphonon model describing charge capture and emission events in the surrounding dielectrics. The charge transfer model is embedded into a drift-diffusion based TCAD simulation environment, which was adapted to 2D devices. Our modeling setup was validated against measurement data on a back-gated single-layer MoS_2 transistor with SiO_2 as a gate dielectric. We use the modeling approach to gain a thorough understanding of the hysteresis, which will help to control this problem in future devices.

INDEX TERMS MOSFET, nanomaterials, semiconductor device modeling, hysteresis, semiconductor device reliability, two-dimensional materials, TCAD modeling.

I. INTRODUCTION

Molybdenum disulfide (MoS_2) is a 2D material of the large group of transition metal dichalcogenides (TMDs), which has received a lot of attention over the past few years. It combines a superior electrostatic control over the channel due to its ultimate thinness, leading to a sufficient suppression of short-channel effects [1], with an inherent, comparatively large transport band gap [2]. This renders it an ideal candidate for applications in digital electronics [3]–[5], as it enables high current on/off ratios and a large transconductance [6].

However, up to now, MoS_2 based field effect transistors (FETs) have not met the high expectations for example when judging device performance in terms of mobilities. When accurately accounting for the non-negligible contact resistances [7], the mobility extracted for MoS_2 layers using multi-terminal measurements at room temperature does not exceed about $100\,cm^2/Vs$ [8]. Besides that, while this mobility value lies in a range comparable with standard silicon technology, the large variability observed in the device characteristics and performance issues like the frequently observed hysteresis in the gate transfer ($I_D(V_G)$) characteristics [9]–[13] and the typically large drifts of the threshold voltage (V_{th}) over time [14] remain critical obstacles inhibiting industrial applications of MoS_2 FETs.

Complementing our previous experimental works on the hysteresis and drift of 2D FETs [14]–[16], here we present a detailed study on the main mechanisms governing the hysteresis phenomenon in the $I_D(V_G)$ characteristics of MoS_2 FETs. Our study is based on a drift-diffusion TCAD model [17], which is adapted to 2D devices in the first part of this paper using experimental results to test our model.

In the second part the degradation of the devices due to charge trapping in the underlying gate dielectric is discussed by coupling the model to a four-state non-radiative multiphonon (NMP) model [18]. This model was originally developed and established for charge transfer reactions in silicon (Si) technologies [19], [20] and is applied here to

2168-6734 © 2018 IEEE. Translations and content mining are permitted for academic research only.
Personal use is also permitted, but republication/redistribution requires IEEE permission.
See http://www.ieee.org/publications_standards/publications/rights/index.html for more information.

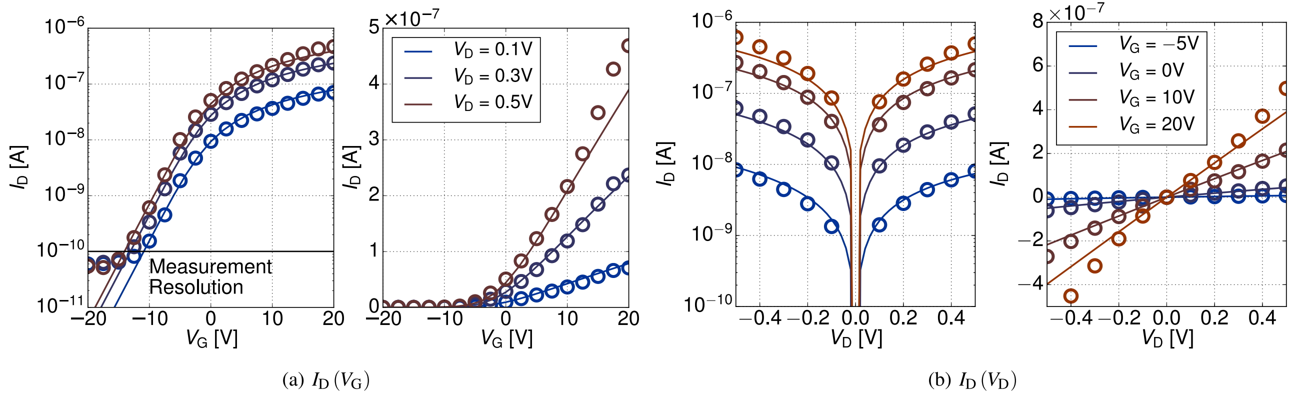

(a) $I_D(V_G)$ (b) $I_D(V_D)$

FIGURE 1. Comparison of measured transfer characteristics (a) and output characteristics (b) (circles) to the simulated curves (solid lines). Excellent agreement between model and data is obtained.

devices based on 2D materials such as MoS_2. Our results confirm that the ubiquitous charge trapping at oxide traps is the main reason for the hysteresis in MoS_2 FETs [14] and provide new insights into the details on the occurrence of a hysteresis. We demonstrate that the hysteresis is caused by the same defect bands in silicon dioxide (SiO_2) that also govern the degradation in silicon devices. However, the degradation in MoS_2-based devices is more pronounced due to the unfavorable band alignment of the SiO_2 defect bands to the band edges of MoS_2.

II. DEVICES AND MEASUREMENTS

A description of the device fabrication and measurement techniques we use here to calibrate our model have been reported in detail elsewhere [14]. For the sake of completeness, we give a short summary of the details which will be important for understanding the simulation results later on. We study a back-gated MoS_2 FET on a 90 nm thick thermal SiO_2 serving as a back gate dielectric. The FET consists of a single layer (SL) flake of MoS_2 (around 6.5 Å), obtained via mechanical exfoliation and selection in an optical microscope [21]. The titanium/gold (Ti/Au) electrodes for the source and drain contacts were deposited using electron beam lithography and metal evaporation [9], forming a device with the dimensions $W = 6.8\,\mu m$ and $L = 1\,\mu m$. As a final fabrication step, the device was annealed in vacuum for 12 hours ($< 5 \times 10^{-6}$ Torr, $T = 120\,°C$) in order to reduce the contact resistances and to remove adsorbed impurities. For a basic electrical characterization the $I_D(V_G)$ characteristics as well as the $I_D(V_D)$ characteristics of the MoS_2/SiO_2 FET were measured using a gate voltage range of $V_G \in [-20\,V,\ 20\,V]$ and a drain voltage range of $V_D \in [0.1\,V,\ 0.5\,V]$ at a temperature of 25 °C in vacuum ($< 1 \times 10^{-5}$ Torr). To thoroughly analyze the hysteresis in the transfer characteristics, several $I_D(V_G)$s were recorded using a varying sweep rate $S = \Delta V/\Delta t$ (with ΔV as the voltage step and Δt as the time step), which corresponds to a sweep frequency of $f = 1/2t_{sw}$ with t_{sw} being the sweep time for one up- or down-sweep. The sweep time was varied in the range of $t_{sw} \in [8\,s,\ 200\,s]$. While the sweep time t_{sw} is an important parameter since it determines the time scale on which the hysteresis occurs, the primary property of the voltage step size ΔV is that it limits the measurement resolution of the hysteresis widths.

III. SIMULATION OF INITIAL DEVICES

In this section the general simulation methodology using drift-diffusion based TCAD [17] is verified against measured characteristics. The drift-diffusion equations [22] can be used because the lateral dimensions of our devices are in the micrometer range ($W \times L \approx 7.0\,\mu m^2$ for the device discussed here). As a consequence, there is a large number of scattering centers in the channel region resulting in scattering-dominated drift-diffusion charge transport. In several recent works [23]–[25] compact models describing devices based on 2D channel materials with drift-diffusion equations have been developed. The usage of drift-diffusion based TCAD has many advantages, among them a high computational efficiency [26] and a good adaptability to variations in device design.

The agreement between measurement and simulation obtained with our method is presented in Fig. 1. Our model is able to capture all aspects of the $I_D(V_G)$ and the $I_D(V_D)$ characteristics on a logarithmic scale as well as on a linear scale.

Critical for this good agreement is the correct choice of material parameters which are given in Table 1. The list of parameters is divided into two sections. The first section contains material constants which are extracted from the band structure calculated with density functional theory. The band structure of TMDs in the single-layer form has been studied in detail by the group of Thygesen [2], [27], [28], [30], [33], [39]. The shape of the band structure and thus also the parameters of this section depend on the dielectric surroundings and the layer number [39], thus the data in Table 1 refers only to the case of SL- MoS_2 on SiO_2.

The second section contains material parameters which are strongly influenced by defects in the channel region and are therefore processing dependent or which are determined by

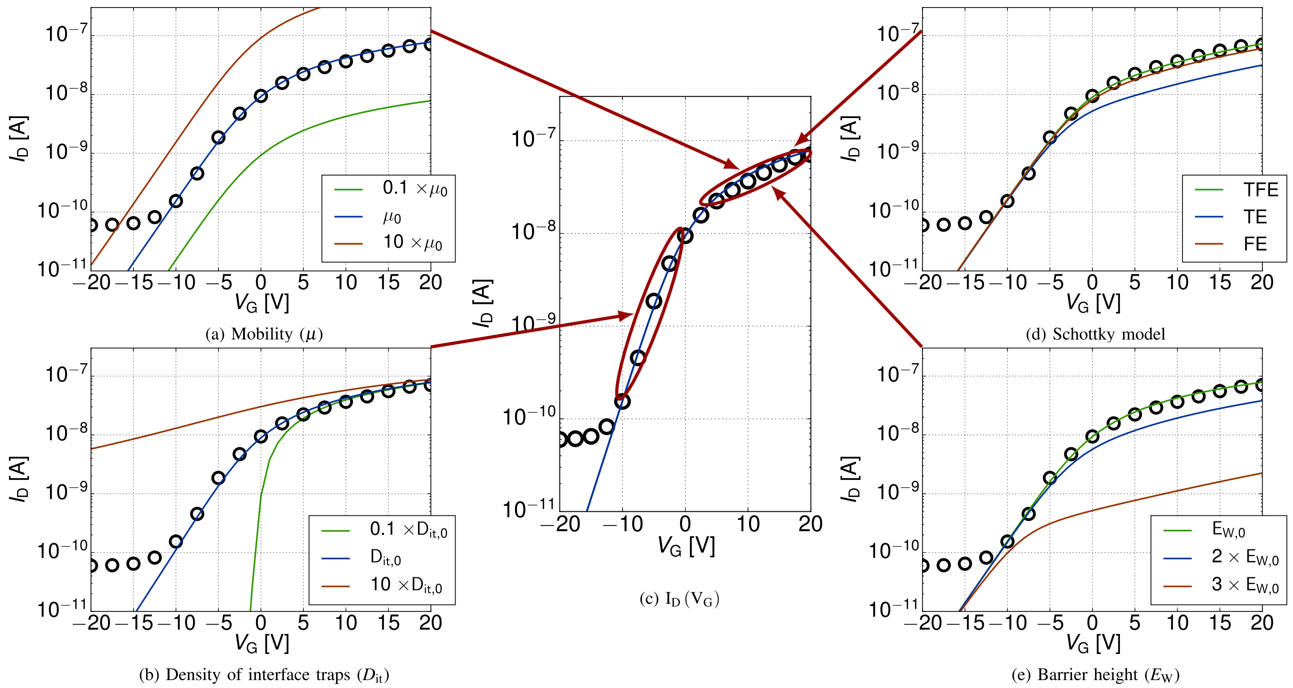

FIGURE 2. **The impact of the most important simulation parameters on the $I_D(V_G)$ characteristic. In the center (c) the fit of the drift-diffusion based TCAD model (solid curve) to the measured data (black circles) is shown. The material properties which are varied on the left hand side (mobility (a) and density of interface traps (b)) are related to the defects in the channel. On the right hand side (Schottky model (d) and barrier height (e)) the impact of contact-related parameters is illustrated.**

TABLE 1. **Material parameters of SL-MoS_2 on SiO_2 serving as input parameters for drift-diffusion based TCAD simulations. The parameters in the first section are extracted from band structures calculated with density functional theory, the parameters in the second section depend strongly on the defects in the semiconductor and thus on the processing conditions.**

Parameter	Value/Range	Reference
Transport band gap (E_G)	2.2 ± 0.1 eV	[2, 27–30]
Electron affinity (χ)	-3.85 ± 0.09 eV	[2, 27, 28, 30, 31]
Electron mass (m_n^*)	0.55 ± 0.05	[2, 32]
Hole mass (m_p^*)	0.56 ± 0.05	[2, 32]
Eff. rel. permittivity (ε_r^{eff})	5.5 ± 0.9	[33, 34]
Work func.diff.(Ti/Au) (E_W)	[0.05, 0.2] eV	[35, 36]
Mobility (μ)	[0.1, 100] cm^2/Vs	[7, 8, 37]
Den. of interface traps (D_{it})	$[10^{12}, 10^{13}]$ $cm^{-2}eV^{-1}$	[38]

the choice and the processing conditions of the metal contacts [7], [35]. For these parameters we only give meaningful ranges according to literature, within which the values should be chosen. At the current stage of research, where there are no generally acknowledged and standardized processing conditions, these parameters have to be treated as fitting values and have to be adjusted to each device separately.

The impact of the most important material parameters on the $I_D(V_G)$ characteristics is illustrated in Fig. 2. The central Fig. 2(c) demonstrates the quality of the established fit and Fig. 2(a) shows the effects of the mobility. The mobility (μ) is degraded by impurities in the channel, which act as scattering centers and determine the overall current level (Fig. 2(a)). While the mobility is the most important parameter of the drift-diffusion model, the impact of interface defects was considered by using the standard Shockley-Read-Hall (SRH) model [40], coupled to the drift-diffusion based TCAD simulator [17]. The density of interface traps (D_{it}) strongly affects the subthreshold slope (Fig. 2(b)). This parameter has been studied in detail by Takenaka *et al.* [38], who associated the typical density of interface traps observed for MoS_2 FETs with sulfur vacancies in the MoS_2 layers.

Contrary to standard CMOS devices, MoS_2 FETs are accumulation devices and the switching process is governed by the modulation of the Schottky barriers at source and drain [41], [42]. The work function difference between the metal contacts and the MoS_2 layer is an important parameter as it defines the Schottky barrier height. The impact of the work function difference is illustrated in Fig. 2(e), demonstrating that already small variations of this parameter can decrease the saturation current level ($I_{D,sat}$) by several orders of magnitude.

In Fig. 2(d) the impact of different models for describing the current transport across Schottky barriers is shown. In general one distinguishes between thermionic emission (TE), thermionic-field emission (TFE) and field emission (FE), depending on whether the thermionic current over the barrier or the tunneling current through the barrier dominates [43], [44]. The TFE model, where the total current over the Schottky barrier is given by the sum of the thermionic component and the tunneling component is the most accurate model and was used in our work. It was

stated previously [7], [45] that the reduced Schottky barrier width in a 2D layer gives rise to large tunneling currents, which is confirmed by Fig. 2(d), where the tunneling component dominates.

In summary, our modeling approach for the characteristics of 2D based devices combines the drift-diffusion equations, which describe the scattering dominated transport through the channel, with a model for the current modulation by the Schottky barriers at source and drain, similar to the one outlined by Appenzeller *et al.* [42] and Penumatcha *et al.* [46]. With this approach a versatile model is obtained, which can serve as a first step towards enabling TCAD-aided device design.

IV. DEFECT MODELING

Having successfully developed a model to describe the current through a fresh device we now take the next step towards modeling the hysteresis. In order to see a shift in the threshold voltage between the up sweep and the down sweep of an $I_D(V_G)$ curve, there has to be charge trapping in the vicinity of the channel. While several groups claim that charge trapping takes place at the interface [12], [47], [48], we argue here in accordance with our previous works [14]–[16] that the fact that the largest hysteresis is observed for the largest sweep time is a strong argument in favor of oxide traps, as they usually have larger time constants than interface traps. For example, according to the SRH model with a band gap of 2.2 eV SL-MoS_2 provides a maximum time constant of 1 µs for a typical capture cross section of $1 \times 10^{-15}\,cm^2$.

Moreover, oxide traps are located at a finite distance from the interface, the most important ones for the charge transfer processes lying typically within the first few nanometers [49]. This leads to an increased bias dependence, as observed in the hysteresis in MoS_2 FETs. The enhanced bias dependence of charge trapping in the oxide in comparison to charge trapping at the interface is illustrated in Fig. 3. Interface traps provide trap levels inside the band gap, thus as the Fermi level sweeps across the band gap for increasing gate voltages, the interface traps become discharged. This charging process is five orders of magnitude faster than the sweep time, thereby effectively reducing the subthreshold slope. Once the Fermi level reaches the conduction band edge (roughly at $V_G \approx V_{th}$), it remains pinned there due to the high concentrations of injected electrons. To a first approximation there are no trapping and detrapping events at interface states above threshold voltage, which is confirmed by comparing the charge state of the interface traps in Fig. 3(b) and 3(c). However, for increasingly positive gate voltages, the oxide defect band is bent downwards, leading to more trapping events in the oxide, consistent with the experimentally observed increase in the hysteresis for increased high levels of the gate voltage $V_{G,H}$ [16]. The charge capture and emission events for gate voltages above the threshold voltage cause an effective shift of the whole $I_D(V_G)$, which produces the observed hysteresis.

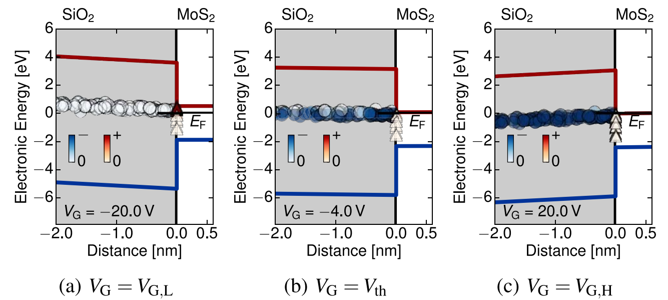

(a) $V_G = V_{G,L}$ (b) $V_G = V_{th}$ (c) $V_G = V_{G,H}$

FIGURE 3. Band diagram of the MoS_2/SiO_2 FET showing the location of donor-like interface traps (red triangles) and of the acceptor-like oxide defect band (blue circles) [50], [51] responsible for the hysteresis. For gate voltages below the threshold voltage, the Fermi level moves through the band gap and interface states become discharged. Above the threshold voltage, the charge state of the interface states remains unchanged and the charging of oxide traps dominates.

For the modeling of the hysteresis we use the four-state non-radiative multiphonon (NMP) model, which accurately describes charge transfer reactions in conventional Si/SiO_2 devices [18]. It does not only account for the energy of the transferred electrons, as it is usually done when using the SRH model [40], but it also considers the energetic relaxation of the structure around the defect, where the electron is captured or emitted [18], [52]. Depending on the microscopic nature of the defect, which has been studied in great detail for SiO_2 based on Si/SiO_2 FETs [53], [54], one usually speaks either of hole or of electron trapping. As the charge transfer process is exactly the same in both cases, the two processes can only be distinguished by the charge change of the trapping defect in the oxide, which either goes from positive to neutral (hole/ donor-like trap) or from neutral to negative (electron/ acceptor-like trap). Therefore, the difference between electron traps and hole traps is only visible in an offset of the transfer characteristic, as it only changes the balance of fixed charges.

Thus, in order to explain the hysteresis in MoS_2 FETs we use the two defect bands of SiO_2 known from silicon technologies [20], [50], [51], with the first being a donor-like hole trapping band located at $\langle E_T^L \rangle \pm \sigma_{E_T^L} = 4.6 \pm 0.3$ eV below the conduction band edge of SiO_2 [20], and the second being an acceptor-like electron trapping band at $\langle E_T^U \rangle \pm \sigma_{E_T^U} = 3.0 \pm 0.2$ eV below the conduction band edge of SiO_2. The second defect band has already been observed for Si-based devices with dielectric gate stacks [50], [51] and has been used in our previous works for the modeling of the hysteresis and of bias-temperature instabilities in FETs based on MoS_2 [14], [16] and black phosphorus [15]. The first defect band is located in the lower half of the band gap of SL-MoS_2 and does not contribute to the degradation in nMOS devices, where the Fermi level only scans across the upper half of the band gap. Therefore, only the second defect band has to be taken into account and is shown in Fig. 3.

Besides the bias dependence of the charge trapping process the second important aspect is the temporal behavior of the responsible defects, as determined by the four-state

NMP model. A trap can only contribute to the hysteresis if it captures an electron at a high gate voltage and emits this electron not before reaching again the low level of the gate voltage. This means that the electron capture time constant (τ_c) of the respective trap has to be smaller than the electron emission time constant (τ_e) at high gate voltages and vice-versa. For this criterion the important voltage level is $V_{th} \approx -4\,V$, where the hysteresis is extracted. If for $V_G < V_{th}$ it holds that $\tau_e < \tau_c$ and for $V_G > V_{th}$ it holds that $\tau_e > \tau_c$, this trap can in principle contribute to the hysteresis.

In Fig. 4(a) and (b) the simulated hysteresis for two different frequencies is shown and compared to measurement data. There were two subsequent measurement rounds to demonstrate that the hysteresis is a reproducible phenomenon and there is no general drift of the characteristics interfering with the hysteresis. Our simulation results clearly corroborate the previously observed [14] PBTI-like hysteresis. PBTI stands for positive bias temperature instability and PBTI-like hysteresis means that the down sweep is shifted to higher threshold voltages just as the threshold voltage is increased under positive stress bias.

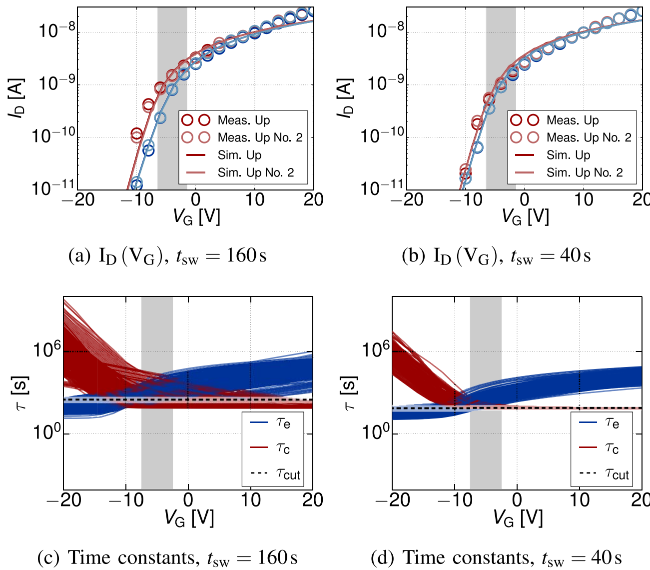

FIGURE 4. Hysteresis fit at two different frequencies (red: up-sweep, blue: down-sweep), together with the voltage dependence of the time constants for a selected set of defects. The sweep time t_{sw} determines the cut-off time via $\tau_{cut} = 2t_{sw}$. At the shorter sweep time, there are fewer defects with time constants in the appropriate range causing a smaller hysteresis width.

When comparing Fig. 4(a) and (b) there is an apparent dependence of the hysteresis width on the sweep frequency. In fact, the traps contributing to the hysteresis at different frequencies are not the same. The time for one up-sweep or one down-sweep ($2t_{sw} = 1/f$) sets to a first approximation an upper limit (τ_{cut}) for the time constants of the contributing traps. If either $\tau_e < \tau_{cut}$ at the maximum negative V_G or $\tau_c < \tau_{cut}$ at maximum positive V_G, this trap can change its charge state for the first time towards the end of the up sweep and for the second time towards the end of the down sweep. If this condition is not fulfilled, it is very unlikely that this trap changes its charge state at all during the sweeping process. In addition, the trap also must not change its charge state too quickly. To be precise, it cannot contribute to the hysteresis if it captures a charge before the hysteresis width is measured at $V_G = V_{th}$. This corresponds to meeting the condition $\tau_c > t(V_{th})$ at threshold voltage, with $t(V_{th})$ being the sweep time until threshold voltage is reached.

In Fig. 4(c) and (d) the bias dependence of the time constants of all traps fulfilling all of the above mentioned criteria and thus causing the hysteresis are displayed. The electron capture time shows a larger bias dependence than the emission time. At shorter sweep times, less defects meet the criteria, reducing the hysteresis width.

To quantify the hysteresis phenomenon, we extracted the hysteresis width at the threshold voltage for all measured sweep frequencies. In Fig. 5 the hysteresis width is shown as a function of the sweep frequency for the measurements and for the simulations. The error bars denote the minimal measurement errors given by the voltage stepping used in the measurements. Additionally, the offset between subsequent measurement rounds is displayed to make sure that no permanent shift of the characteristics interferes with the hysteresis. Good agreement between measured and simulated data is obtained, clearly demonstrating that our simulation methodology captures the time behavior of the hysteresis phenomenon correctly.

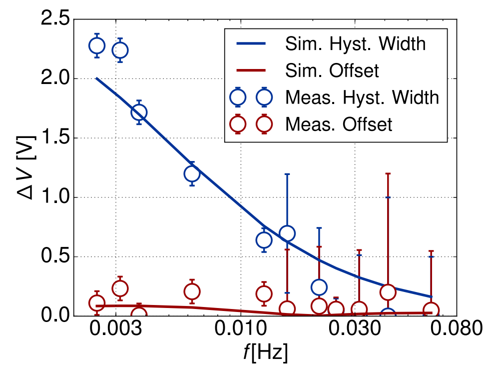

FIGURE 5. Hysteresis width (extracted between up- and down-sweep (blue)) and the offset (extracted between two up- or two down-sweeps for different measurement rounds (red)) as a function of the sweep frequency. The error bars report the minimum error of the measurement process given by the voltage step ΔV used to record the $I_D(V_G)$ curve. The hysteresis width decreases quickly for fast sweeps and there is only a small overall offset, ruling out a dominant general drift.

V. CONCLUSION

A general drift-diffusion based TCAD simulation methodology for devices based on 2D materials such as MoS_2 was established. By coupling a non-radiative multiphonon model to this simulation framework, charge capture events at oxide traps can be described. As oxide traps show a larger bias dependence and larger time constants than interface traps,

we concluded that oxide traps are responsible for the hysteresis observed in the $I_D(V_G)$ characteristics of back-gated SL-MoS_2 FETs. The NMP model correctly captures the sweep time dependence of the hysteresis width, confirming the suitability of our approach.

ACKNOWLEDGMENT

The authors would like to acknowledge inspiring discussions with Gianluca Fiori (University of Pisa), Mario Lanza (Suzhou University) and Dmitry Polyushkin (TU Wien).

REFERENCES

[1] F. Schwierz, J. Pezoldt, and R. Granzner, "Two-dimensional materials and their prospects in transistor electronics," *Nanoscale*, vol. 7, no. 18, pp. 8261–8283, 2015.
[2] F. A. Rasmussen and K. S. Thygesen, "Computational 2D materials database: Electronic structure of transition-metal dichalcogenides and oxides," *J. Phys. Chem. C*, vol. 119, no. 23, pp. 13169–13183, Jun. 2015.
[3] B. Radisavljevic, A. Radenovic, J. Brivio, V. Giacometti, and A. Kis, "Single-layer MoS_2 transistors," *Nat. Nanotechnol.*, vol. 6, no. 3, pp. 147–150, 2011.
[4] G. Fiori *et al.*, "Electronics based on two-dimensional materials," *Nat. Nanotechnol.*, vol. 9, no. 10, pp. 768–779, 2014.
[5] S. Wachter, D. K. Polyushkin, O. Bethge, and T. Mueller, "A microprocessor based on a two-dimensional semiconductor," *Nat. Commun.*, vol. 8, pp. 14948.1–14948.6, Apr. 2017.
[6] Y. Yoon, K. Ganapathi, and S. Salahuddin, "How good can monolayer MoS_2 transistors be?" *Nano Lett.*, vol. 11, no. 9, pp. 3768–3773, 2011.
[7] S. Das, H.-Y. Chen, A. V. Penumatcha, and J. Appenzeller, "High performance multilayer MoS_2 transistors with scandium contacts," *Nano Lett.*, vol. 13, no. 1, pp. 100–105, 2013.
[8] X. Cui *et al.*, "Multi-terminal transport measurements of MoS_2 using a van der Waals heterostructure device platform," *Nat. Nanotechnol.*, vol. 10, no. 6, pp. 534–540, 2015.
[9] D. J. Late, B. Liu, H. S. Matte, V. P. Dravid, and C. N. Rao, "Hysteresis in single-layer MoS_2 field effect transistors," *ACS Nano*, vol. 6, no. 6, pp. 5635–5641, 2012.
[10] T. Li, G. Du, B. Zhang, and Z. Zeng, "Scaling behavior of hysteresis in multilayer MoS_2 field effect transistors," *Appl. Phys. Lett.*, vol. 105, no. 9, 2014, Art. no. 093107.
[11] A.-J. Cho *et al.*, "Multi-layer MoS_2 FET with small hysteresis by using atomic layer deposition Al_2O_3 as gate insulator," *ECS Solid State Lett.*, vol. 3, no. 10, pp. Q67–Q69, 2014.
[12] Y. Park, H. W. Baac, J. Heo, and G. Yoo, "Thermally activated trap charges responsible for hysteresis in multilayer MoS_2 field-effect transistors," *Appl. Phys. Lett.*, vol. 108, no. 8, 2016, Art. no. 083102.
[13] J. Shu *et al.*, "The intrinsic origin of hysteresis in MoS_2 field effect transistors," *Nanoscale*, vol. 8, no. 5, pp. 3049–3056, 2016.
[14] Y. Y. Illarionov *et al.*, "The role of charge trapping in MoS_2/SiO_2 and MoS_2/hBN field-effect transistors," *2D Mater.*, vol. 3, no. 3, pp. 1–11, 2016.
[15] Y. Y. Illarionov *et al.*, "Long-term stability and reliability of black phosphorus field-effect transistors," *ACS Nano*, vol. 10, pp. 9543–9549, Oct. 2016.
[16] Y. Y. Illarionov *et al.*, "Energetic mapping of oxide traps in double-gated MOS_2 field-effect transistors," *2D Mater.*, vol. 4, no. 2, pp. 1–13, 2017.
[17] *Minimos-NT Manual*, Glob. TCAD Solutions, Vienna, Austria, 2017.
[18] T. Grasser, "Stochastic charge trapping in oxides: From random telegraph noise to bias temperature instabilities," *Microelectron. Rel.*, vol. 52, no. 1, pp. 39–70, 2012.
[19] T. Grasser *et al.*, "The paradigm shift in understanding the bias temperature instability: From reaction–diffusion to switching oxide traps," *IEEE Trans. Device Mater. Rel.*, vol. 58, no. 11, pp. 3652–3666, Nov. 2011.
[20] G. Rzepa *et al.*, "Complete extraction of defect bands responsible for instabilities in n and pFinFETs," in *Symp. VLSI Technol. Dig. Tech. Papers*, Honolulu, HI, USA, 2016, pp. 1–2.
[21] M. M. Furchi, A. Pospischil, F. Libisch, J. Burgdörfer, and T. Mueller, "Photovoltaic effect in an electrically tunable van der Waals heterojunction," *Nano Lett.*, vol. 14, no. 8, pp. 4785–4791, 2014.
[22] W. V. Roosbroeck, "Theory of the flow of electrons and holes in germanium and other semiconductors," *Bell Syst. Tech. J.*, vol. 29, no. 4, pp. 560–607, Oct. 1950.
[23] M. G. Ancona, "Electron transport in graphene from a diffusion-drift perspective," *IEEE Trans. Electron Devices*, vol. 57, no. 3, pp. 681–689, Mar. 2010.
[24] D. Jiménez, "Drift-diffusion model for single layer transition metal dichalcogenide field-effect transistors," *Appl. Phys. Lett.*, vol. 101, no. 24, 2012, Art. no. 243501.
[25] S. V. Suryavanshi and E. Pop, "S_2DS: Physics-based compact model for circuit simulation of two-dimensional semiconductor devices including non-idealities," *J. Appl. Phys.*, vol. 120, no. 22, 2016, Art. no. 224503.
[26] M. Lundstrom, "Drift-diffusion and computational electronics—Still going strong after 40 years!" in *Proc. Int. Conf. Simulat. Semicond. Processes Devices (SISPAD)*, Washington, DC, USA, Sep. 2015, pp. 1–3.
[27] K. S. Thygesen, "Calculating excitons, plasmons, and quasiparticles in 2D materials and van der Waals heterostructures," *2D Mater.*, vol. 4, no. 2, 2017, Art. no. 022004.
[28] F. A. Rasmussen, P. S. Schmidt, K. T. Winther, and K. S. Thygesen, "Efficient many-body calculations of 2D materials using exact limits for the screened potential: Band gaps of MoS_2, hBN, and phosphorene," *Phys. Rev. B, Condens. Matter*, vol. 94, no. 15, pp. 1–9, 2016.
[29] H. M. Hill, A. F. Rigosi, K. T. Rim, G. W. Flynn, and T. F. Heinz, "Band alignment in MoS_2/WS_2 transition metal dichalcogenide heterostructures probed by scanning tunneling microscopy and spectroscopy," *Nano Lett.*, vol. 16, no. 8, pp. 4831–4837, 2016.
[30] C. Jin, F. A. Rasmussen, and K. S. Thygesen, "Tuning the Schottky barrier at the graphene/MoS_2 interface by electron doping: Density functional theory and many-body calculations," *J. Phys. Chem. C*, vol. 119, no. 34, pp. 19928–19933, 2015.
[31] V. D. S. Ganesan, J. Linghu, C. Zhang, Y. P. Feng, and L. Shen, "Heterostructures of phosphorene and transition metal dichalcogenides for excitonic solar cells: A first-principles study," *Appl. Phys. Lett.*, vol. 108, no. 12, 2016, Art. no. 122105.
[32] A. Ramasubramaniam, "Large excitonic effects in monolayers of molybdenum and tungsten dichalcogenides," *Phys. Rev. B, Condens. Matter*, vol. 86, no. 11, pp. 1–6, 2012.
[33] S. Latini, T. Olsen, and K. S. Thygesen, "Excitons in van der Waals heterostructures: The important role of dielectric screening," *Phys. Rev. B, Condens. Matter*, vol. 92, no. 24, 2015, Art. no. 245123.
[34] T. C. Berkelbach, M. S. Hybertsen, and D. R. Reichman, "Theory of neutral and charged excitons in monolayer transition metal dichalcogenides," *Phys. Rev. B, Condens. Matter*, vol. 88, no. 4, 2013, Art. no. 045318.
[35] A. Allain, J. Kang, K. Banerjee, and A. Kis, "Electrical contacts to two-dimensional semiconductors," *Nat. Mater.*, vol. 14, no. 12, pp. 1195–1205, 2015.
[36] S. McDonnell, C. Smyth, C. L. Hinkle, and R. M. Wallace, "MoS_2-titanium contact interface reactions," *ACS Appl. Mater. Interfaces*, vol. 8, no. 12, pp. 8289–8294, 2016.
[37] S. Chuang *et al.*, "MoS_2 P-type transistors and diodes enabled by high work function MoOx contacts," *Nano Lett.*, vol. 14, no. 3, pp. 1337–1342, 2014.
[38] M. Takenaka, Y. Ozawa, J. Han, and S. Takagi, "Quantitative evaluation of energy distribution of interface trap density at MoS_2 MOS interfaces by the Terman method," in *Proc. IEEE Int. Electron Devices Meeting*, San Francisco, CA, USA, 2016, pp. 139–142.
[39] K. T. Winther and K. S. Thygesen, "Quasiparticle band structure engineering in van der Waals heterostructures via dielectric screening," *2D Mater.*, vol. 4, May 2017, Art. no. 025059.
[40] W. Shockley and W. T. Read, "Statistics of the recombination of holes and electrons," *Phys. Rev.*, vol. 87, no. 46, pp. 835–842, 1952.
[41] H. Liu *et al.*, "Switching mechanism in single-layer molybdenum disulfide transistors: An insight into current flow across Schottky barriers," *ACS Nano*, vol. 8, no. 1, pp. 1031–1038, 2014.
[42] J. Appenzeller, F. Zhang, S. Das, and J. Knoch, "Transition metal dichalcogenide Schottky barrier transistors," in *2D Materials for Nanoelectronics*, vol. 17. Boca Raton, FL, USA: CRC Press, 2016, ch. 8, pp. 207–234.
[43] E. H. Rhoderick and R. Williams, *Metal-Semiconductor Contacts*. Oxford, U.K.: Clarendon Press, 1978.
[44] D. Schroeder, *Modelling of Interface Carrier Transport for Device Simulation*. Vienna, Austria: Springer, 1994.
[45] J. Appenzeller *et al.*, "Toward nanowire electronics," *IEEE Trans. Electron Devices*, vol. 55, no. 11, pp. 2827–2845, Nov. 2008.

[46] A. V. Penumatcha, R. B. Salazar, and J. Appenzeller, "Analysing black phosphorus transistors using an analytic Schottky barrier MOSFET model," *Nat. Commun.*, vol. 6, p. 8948, Jun. 2015.
[47] Y. Guo *et al.*, "Charge trapping at the MoS_2-SiO_2 interface and its effects on the characteristics of MoS_2 metal-oxide-semiconductor field effect transistors," *Appl. Phys. Lett.*, vol. 106, no. 10, 2015, Art. no. 103109.
[48] K. Choi *et al.*, "Trap density probing on top-gate MoS_2 nanosheet field-effect transistors by photo-excited charge collection spectroscopy," *Nanoscale*, vol. 7, no. 13, pp. 5617–5623, 2015.
[49] B. E. Deal, "Standardized terminology for oxide charges associated with thermally oxidized silicon," *IEEE Trans. Electron Devices*, vol. ED-27, no. 3, pp. 606–608, Mar. 1980.
[50] R. Degraeve *et al.*, "Trap spectroscopy by charge injection and sensing (TSCIS): A quantitative electrical technique for studying defects in dielectric stacks," in *Int. Electron Devices Meeting Tech. Dig. (IEDM)*, San Francisco, CA, USA, 2008, pp. 10–13.
[51] G. Rzepa *et al.*, "Efficient physical defect model applied to PBTI in high-k stacks," in *Proc. IEEE Int. Rel. Phys. Symp. (IRPS)*, Monterey, CA, USA, 2017, pp. XT-11.1–XT-11.6.
[52] C. B. Layne, W. L. Lowdermilk, and M. J. Weber, "Multiphonon relaxation of rare-earth ions in oxide glasses," *Phys. Rev. B, Condens. Matter*, vol. 16, no. 1, pp. 10–20, 1977.
[53] T. Grasser *et al.*, "On the microscopic structure of hole traps in pMOSFETs," in *Proc. IEEE Int. Electron Devices Meeting*, San Francisco, CA, USA, 2014, pp. 21.1.1–21.1.4.
[54] Y. Wimmer, A.-M. El-Sayed, W. Gös, T. Grasser, and A. L. Shluger, "Role of hydrogen in volatile behaviour of defects in SiO_2-based electronic devices," *Proc. Roy. Soc. A Math. Phys. Eng. Sci.*, vol. 472, no. 2190, 2016, Art. no. 20160009.

THERESIA KNOBLOCH received the B.Sc. degree in technical physics and the Diplomingenieur degree in microelectronics from TU Wien, Vienna, Austria, in 2014 and 2016, respectively. Currently, she is pursuing the Doctoral degree with the Institute for Microelectronics, focusing on degradation effects observed in 2D devices. Her research interests span from general modeling issues arising out of the two-dimensionality to variability and reliability studies on this novel device class. In 2017, she visited Soochow University, China, where she fabricated MoS_2-based devices.

GERHARD RZEPA received the B.Sc. degree in electrical engineering and the Diplomingenieur degree in microelectronics from TU Wien (Vienna University of Technology) in 2010 and 2013, respectively, where he is currently pursuing the Doctoral degree with the Institute for Microelectronics. His current research interests include oxide degradation, device variability and measuring and modeling of related reliability phenomena, such as bias temperature instabilities, hot carrier degradation, random telegraph noise, and stress induced leakage currents.

YURY YU ILLARIONOV was born in Leningrad (currently Saint-Petersburg) in 1988. He received the B.Sc. and M.Sc. degrees from St.-Petersburg State Polytechnical University, Russia, in 2009 and 2011, respectively, the double Erasmus Mundus M.Sc. degrees from Grenoble INP, France, and the University of Augsburg, Germany, in 2012, the Ph.D. degree in semiconductor physics from Ioffe Physical-Technical Institute in 2015, and the Dr.techn. degree from TU Wien in 2015. His scientific carrier started in 2007 in Ioffe Physical-Technical Institute, Russia, and in 2011, where he joined the Ph.D. program. He also visited IRCELYON, France, in 2011, for two months, and the Singapore Institute of Manufacturing Technology, Singapore, in 2012, for six months, as a young Guest Researcher. In 2013, he joined the Institute for Microelectronics, TU Wien, Austria. In 2018, he is a Post-Doctoral Researcher working on reliability of the next-generation 2D FETs with graphene, MoS_2, and black phosphorus. He coauthored over 60 research contributions in scientific journals (including ACS Nano, 2D Materials, and Applied Physics Letters) and conference proceedings.

MICHAEL WALTL received the Ph.D. degree from TU Wien, Vienna, Austria, in 2016, where he currently leads the Technology Characterization Laboratory with the Institute for Microelectronics. His current research interests include the experimental characterization of reliability issues in semiconductor devices and more exotic devices employing 2D materials.

FRANZ SCHANOVSKY received the Ph.D. degree in microelectronics from TU Wien in 2013, where he focused on the atomistic modeling of the bias temperature instability in MOS transistors. After working as a Post-Doctoral Researcher and a Software Developer, he joined GTS as a Senior Researcher in 2016. He is responsible for the extension and development of the reliability and variability models in the Minimos-NT device simulator.

BERNHARD STAMPFER was born in Austria in 1989. He received the B.Sc. degree in electrical engineering and the Diplomingenieur degree in microelectronics and photonics from TU Wien, Vienna, Austria, in 2013 and 2016, respectively, where he is currently pursuing the Doctoral degree with the Institute for Microelectronics. His research interests include device reliability, oxide and interface trapping, electrical methods of defect characterization (TDDS, random telegraph noise, CV measurements), and defect simulation.

MARCO M. FURCHI received the Ph.D. degree from the Photonics Institute of TU Wien, Vienna, Austria, in 2016, where he was a Post-Doctoral Researcher. In 2015, he was a Visiting Researcher with MIT (Department of Physics), Cambridge, MA, USA. His research activities were focused on optical and electrical properties of graphene and atomically thin transition metal dichalcogenides.

THOMAS MUELLER received the Ph.D. degree in electrical engineering from TU Vienna in 2004. In 2007, he joined the IBM Watson Research Center, USA, as a Post-Doctoral, working on carbon-based optoelectronics. In 2009, he returned to TU Vienna, where he currently holds an Associate Professor position. His research focuses on electronic and optoelectronic devices based on 2D materials. He (co-)authored over 80 peer-reviewed publications in leading scientific journals. Selected awards include the START-Prize, the Fritz Kohlrausch-Prize, and the ASciNA Award.

TIBOR GRASSER is the Head of the Institute for Microelectronics, TU Wien. He has edited various books, e.g., on the bias temperature instability and hot carrier degradation (both Springer), is a Distinguished Lecturer of the IEEE EDS, has been involved in outstanding conferences, such as IEDM, IRPS, SISPAD, ESSDERC, and IIRW. He was a recipient of the Best and Outstanding Paper Awards at IRPS in 2008, 2010, 2012, and 2014, the IPFA in 2013 and 2014, and the ESREF in 2008, and the IEEE EDS Paul Rappaport Award in 2011.